Available online at www.sciencedirect.com
SCIENCE DIRECT®
ELSEVIER
Journal of Crystal Growth 250 (2003) 262–268
JOURNAL OF CRYSTAL GROWTH
www.elsevier.com/locate/jcrysgro

Detection of trace water in phosphine with cavity ring-down spectroscopy

Susan Y. Lehman[a,*], Kris A. Bertness[a], Joseph T. Hodges[b]

[a] National Institute of Standards and Technology, Mailcode 815.04, 325 Broadway, Boulder, CO 80305-3328, USA
[b] National Institute of Standards and Technology, 100 Bureau Drive, Stop 8363, Gaithersburg, MD 20899-8363, USA

Abstract

Water is a detrimental impurity even at concentrations of 10 nmol/mol or less in source gases for compound semiconductor epitaxial growth. Oxygen complexes from water incorporation cause degraded luminescent efficiency and reduced minority-carrier lifetimes. Most techniques for detecting water in process gases have poor accuracy below 1 μmol/mol and require frequent calibration and control of ambient humidity. Cavity ring-down spectroscopy (CRDS), in contrast, makes use of a fundamental physical property of H_2O molecules—the optical absorption line strength—and a time-constant measurement to provide a water concentration value with high precision and low uncertainty even in the nmol/mol range. We describe the CRDS technique and present the first CRDS measurements of trace H_2O contamination in unpurified and purified phosphine. We also report secondary-ion mass spectrometry measurements of the O concentration profiles within a multi-layer film grown using molecular-beam epitaxy in which respective film layers were grown with the purified and unpurified phosphine previously characterized by CRDS.
© 2002 Elsevier Science B.V. All rights reserved.

PACS: 33.20.Ea; 39.30.+w; 81.05.Ea; 68.55.Ln

Keywords: A1. Cavity ring-down spectroscopy; A1. Impurities; A3. Molecular beam epitaxy; B1. Phosphides; B2. Semiconducting aluminum compounds; B2. Semiconducting III–V materials

1. Introduction

The detection of impurities in semiconductor source gases is of interest because of the detrimental effects that impurities may have on the optoelectronic properties of the final material. In particular, water and molecular oxygen tend to form oxygen complexes with energies deep in the band gap of the resultant semiconductor. These deep-level impurities cause non-radiative recombination of electrons and holes, leading to lower efficiencies and noisier device performance. Aluminum-containing compounds are particularly sensitive to oxidation. Although purifiers are available to remove most H_2O from semiconductor source gases, the remaining H_2O concentration is typically below the detection limits of standard techniques such as Fourier-transform infrared spectroscopy (FTIR) and frost-point hygrometry [1,2]. As device manufacturers seek to improve their products through the use of higher-purity gases, more sensitive methods for measuring such trace quantities of H_2O are needed.

*Corresponding author. Tel.: +1-303-497-7554; fax: +1-303-497-3387.
E-mail address: slehman@boulder.nist.gov (S.Y. Lehman).

0022-0248/03/$ - see front matter © 2002 Elsevier Science B.V. All rights reserved.
doi:10.1016/S0022-0248(02)02248-0

The purpose of this work is to quantify the correspondence between the content of H_2O in source gases and the quality of resultant semiconductor films. The general approach is to combine advanced capabilities for quantification of trace H_2O in source gases with existing methods of film growth and characterization. In this study, we used cavity ring-down spectroscopy (CRDS), a high-sensitivity method based on optical absorption, to measure the residual H_2O content of the source gas (phosphine), and we measured the correlation between this H_2O and the amount of O incorporated within AlInP structures grown via molecular-beam epitaxy (MBE).

2. Cavity ring-down spectroscopy

CRDS [3,4] is a relatively new technique in which the absorption coefficient of a gas sample is obtained directly from measurements of the decay of radiant power circulating inside a high-finesse cavity similar to a Fabry–Pérot interferometer. The resonating cavity is composed of two curved dielectric mirrors, separated by a distance a, forming a stable optical resonator. Following the abrupt termination of the laser excitation of frequency ν, the optical power leaking out of the ring-down cavity through the transmission of the back mirror is measured with a fast detector. The CRDS signal is a simple exponential decay characterized by the ring-down cavity decay time constant τ. The decay time constant $\tau(\nu)$ is inversely proportional to the sum of all single-pass losses within the cavity, $L_{\mathrm{tot}}(\nu)$, and is given by

$$\tau(\nu) = \frac{a}{c}\frac{1}{L_{\mathrm{tot}}(\nu)}, \tag{1}$$

where c is the speed of light in the medium within the cavity. This equation represents the observed absorption spectrum, determined solely by measuring the cavity decay time constant as a function of frequency, and is valid provided $L_{\mathrm{tot}}(\nu) \ll 1$ (a condition that is typically met for CRDS experiments using ultra-low-loss super-polished dielectric mirrors).

The sources of losses in the cavity include the mirror loss and Rayleigh scattering and, depending on the frequency of light and the material in the cavity, may also include optical absorption by the material in the cavity. Thus, the ring-down time changes when light-absorbing impurities are present in the cavity, as shown in Fig. 1. By integrating the total cavity loss over the measured frequency range and assuming the individual line shape function for optical absorption to be well-represented by a Voigt profile [5], we then find that

$$\int L_{\mathrm{tot}}(\nu)\,\mathrm{d}\nu = \int L_{\mathrm{base}}(\nu)\,\mathrm{d}\nu + an\sum x_i \sum S_{ik}, \tag{2}$$

where x_i represents the mole fraction of species i, S_{ik} is the line strength of the kth molecular absorption transition of species i occurring at a particular frequency ν_{ik}, and the total number density of the gas mixture is $n = P(k_{\mathrm{b}}T)^{-1}$. P and T are, respectively, the total cell pressure and temperature and k_{b} is the Boltzmann constant. The base loss of the ring-down system L_{base} can

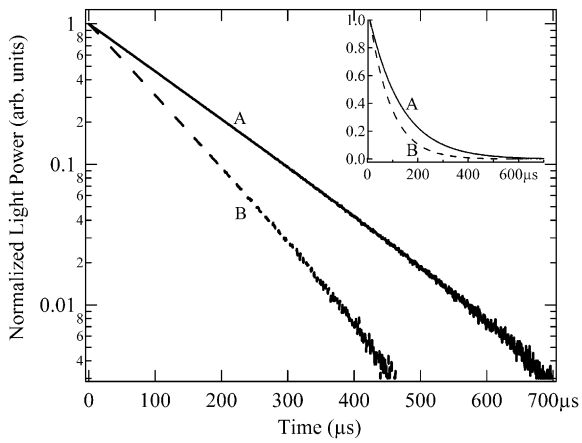

Fig. 1. Normalized ring-down signals exhibiting the characteristic exponential decay of light power that occurs after the cavity is pumped with light and the excitation laser is switched off. This rate of decay depends on the mirror losses, which are constant, and on absorption losses, which depend on the amount and type of absorbing material present in the cavity, the frequency of the light, and the absorption line strength. In trace A water was present in the cavity, but the laser frequency did not overlap any absorption transitions. In trace B the frequency did overlap an absorption transition, leading to a more rapid decay of the light in the cavity. The inset displays the same data on linear axes. The curvature at long times is associated with a non-zero baseline.

Table 1
Transition wavenumbers, wavelengths and line strengths [7,8] for the water absorption lines used in the current CRDS measurements

Label	$\tilde{\nu}$ (cm^{-1})	Transition wavelength (nm)	S_{water} (cm^2 MHz/molecule)	S_{water} ($cm^2\,cm^{-1}$/molecule)	anS_{water} (MHz)
Weak line	10 686.32	935.776262	3.48×10^{-19}	1.16×10^{-23}	85.1
Strong line	10 687.36	935.684509	2.05×10^{-17}	6.83×10^{-22}	5013

Note: The line strengths are reported both in SI and spectroscopic units. The quantity anS_{water} is based on a cavity length $a = 75$ cm, sample pressure $P = 13.3$ kPa (100 Torr), and temperature $T = 296$ K.

usually be treated as a slowly varying linear function over the spectral range considered, and consequently the measured CRDS spectra can be modeled as the sum of Voigt profiles and a slowly varying baseline. In the case where only a single absorption transition of H_2O, denoted by S_{water}, is present in the measured spectral range, the mole fraction of H_2O, x_w, is given by

$$x_w = A_{Voigt}/anS_{water}, \tag{3}$$

where A_{Voigt} is the area of the single Voigt profile given by a least-squares fit to the observed spectrum.

Eq. (3) illustrates one of the unique features of CRDS, namely that it does not require calibration in the conventional sense. Alternative methods of determining impurity concentrations can be affected by drift in detector sensitivity, illumination source power, and transparency of windows and other optical elements. Calibration of such instruments is required and utilizes "known" gas mixtures, but this method of calibration is particularly problematic with water, where the concentration in the gas is altered by transport through tubing and is rarely stable over time. For CRDS, the sources of uncertainty can be determined directly for the experimentally derived parameters in Eq. (3), and therefore calibration per se is not necessary. For a more detailed discussion of the combined uncertainty of the cavity ring-down technique, see Ref. [6], in which transition line strengths for O_2 were measured to a precision of better than 0.5%.

Two H_2O absorption transitions (having an approximately 50-fold difference in line strength) were probed in this study. Values from the most recent spectral line database [7,8] have been used for these transition line strengths. Uncertainties were not reported for individual lines, but are reported overall as 2.5–5%; ongoing measurements of the H_2O line strengths utilizing primary thermodynamic-based standards of humidity generation [9] will lead to lower uncertainties in these line strengths. The respective transition frequencies (expressed as the wavenumber $\tilde{\nu} = c\nu$), wavelengths, line strengths and the quantities anS_{water} (at the nominal pressure and temperature conditions of these experiments) for these H_2O absorption lines are given in Table 1. The uncertainties in concentration reported here are standard uncertainties (i.e., one standard deviation) and represent uncertainties in the fit-derived Voigt area, temperature and pressure.

3. Experimental procedure

The ring-down system is composed of a symmetric ring-down cavity with mirrors of nominal reflectivity 0.999985 mounted in an evacuatable volume. The internal surfaces are all electropolished stainless-steel tubing, and the internal volume of the system is approximately 0.2 L. A piezoelectric transducer is used for precise translation of one cavity mirror, thus enabling the consistent excitation of a specific cavity mode as the laser frequency is tuned. A tunable, continuous-wave, single-mode external cavity diode laser emitting in the spectral range 920–940 nm is used as a probe laser. A wavemeter is used to determine the laser frequency (uncertainty of <1000 MHz) and tune the laser to known H_2O absorption transitions. During a spectral scan a scanning étalon with a resolution <10 MHz is used to measure the frequency steps of the laser. The laser output is passed through an acousto-optic

modulator (AOM), and the first-order beam deflected by the AOM is used to pump the ring-down cavity. The passive decay of light from the ring-down cavity is initiated by switching the drive power to the AOM, yielding an effectively instantaneous turn-off of the probe laser. Ring-down signals are measured by use of an Si-PIN photodetector with 200 kHz bandwidth. Spectral scans are achieved by tuning the diode laser frequency through sequential longitudinal modes of the fundamental transverse mode of the length-stabilized cavity.

The ring-down cavity system has been constructed adjacent to an MBE machine, which is supplied by the same phosphine source and lines as the cavity, enabling gas-source MBE growth using well-characterized phosphine gas. CRDS measurements were normally made with a nominal gas flow rate of 10 standard cm^3/min and nominal cavity pressure of 13.3 kPa (100 Torr). The water concentration of phosphine (PH_3) gas samples from two different cylinders was measured. Phosphine cylinder *A* was nearly 4 years old and more than 2 years beyond its quoted shelf life when its water concentration was measured with the ring-down cavity. Phosphine cylinder *B* was well within its specified shelf life when gas from it was tested. The in-line phosphine purifier is filled with a chemically reactive material that reacts with water to remove it from the gas. The purifier was replaced at the same time that cylinder *B* was installed. The term "unpurified phosphine" is used below to describe gas directly from the cylinder, while "purified phosphine" refers to gas that has passed through the in-line purifier.

To test the quality of material grown with this phosphine, a structure with two layers of $Al_{0.58}In_{0.42}P$ 1.5 μm thick separated by a 200 nm layer of GaAs was grown using purified and unpurified phosphine for the respective AlInP layers. Before beginning the layer grown with purified phosphine, a quantity of purified phosphine equivalent to nine times the line volume between the purifier and the growth chamber was allowed to flow through the line and vented. During the GaAs spacer layer growth, the purifier was switched out of the line and a quantity of phosphine equal to three times the line volume was vented to ensure that the top layer was grown with truly unpurified phosphine. The structure was capped with 200 nm GaAs, and all layers were doped p-type with Be. This growth was done with phosphine from cylinder *B*.

4. Results

Before measuring the water concentration of cylinder *A*, the cavity was sealed and purged by flowing dry nitrogen until the background water concentration in the cavity was measured by CRDS as 0.19 ± 0.03 μmol/mol (0.19 μmol H_2O per mole of gas; also frequently reported as 0.19 ppm). The line to the phosphine cylinder was then evacuated to below 130 Pa (<1 Torr) before charging the line with phosphine. The initial charge of phosphine was vented at 55 standard cm^3/min for 30 min before the phosphine was allowed to flow through the ring-down cavity. Due to the pressure drifting in the ring-down cell, the cylinder *A* phosphine sample was measured as a static charge instead of under flowing conditions. Probing the weak water absorption line at $10686.32\,cm^{-1}$, we found a concentration of 730 ± 60 μmol/mol water in the cylinder *A* phosphine. This level of water is considerably above the manufacturer's specifications of 1 μmol/mol for the cylinder.

To confirm that this high water concentration originated with the phosphine gas, and not the cavity walls or lines, we acquired additional data in nitrogen delivered to the cavity from the purge cylinder in the phosphine gas cabinet. As mentioned above, before filling the cavity with phosphine, CRDS measurements gave a water vapor mole fraction of approximately 0.19 μmol/mol. The static charge of phosphine remained in the cavity for 3 h during the CRDS measurements probing the weak water line given in Table 1, after which the cavity was evacuated once and immediately filled with dry nitrogen. The cavity was deliberately not purged so as to assess the worst-case outgas rate, even though the nitrogen charge therefore would absorb water left behind by the wet phosphine. This static charge of nitrogen was kept in the cavity for more than 45 h and was

measured with both the strong and weak water absorption lines a total of three times. Over this time, the quantity of water in the cavity did rise slightly due to outgassing—from 43 ± 2 μmol/mol at 18 h to 80 ± 4 μmol/mol at 45 h. This outgassing rate of 1.4 ± 0.1 (μmol/mol)/h is more than an order of magnitude smaller than the rate of 24 (μmol/mol)/h that would be necessary to explain the high water concentration of the phosphine by outgassing.

As noted, this water mole fraction of 730 ± 60 μmol/mol is above the manufacturer's specifications. However, the cylinder was well beyond the quoted expiration date. Water concentrations in ammonia cylinders have been observed to rise as the cylinder is used over time [10] and something similar likely occurred in this cylinder. However, since we did not measure the water concentration of the phosphine in this cylinder earlier in its life, we cannot rule out that it had a high water concentration when first received. Due to the high water content of cylinder *A*, both the cylinder and in-line purifier were replaced.

Figs. 2 and 3 present the results of a unified set of CRDS measurements of water in nitrogen and phosphine, respectively. Before measuring the water concentration of phosphine cylinder *B*, the cavity was purged with flowing nitrogen for 24 h. The background concentration of water was then 1.4 ± 0.2 μmol/mol; this CRDS spectrum is shown as trace *A* in Fig. 2. The same evacuation of the phosphine line and venting of the initial phosphine sample as described above was then performed. Flowing purified phosphine was then analyzed with CRDS (trace *B*, Fig. 3). Finally, the purifier was bypassed and flowing unpurified phosphine was measured (trace *A*, Fig. 3). These three measurements were taken within a few hours of each other.

After these measurements, the cavity was purged with several cycles of evacuation and backfilling with nitrogen. The cavity was also heated to $\cong 40$°C to promote the outgassing of residual water from the walls. After this purging and baking, the background mole fraction of water was reduced to 0.15 ± 0.03 μmol/mol, calculated from the CRDS spectrum shown as trace *B* in Fig. 2. The purified phosphine was then

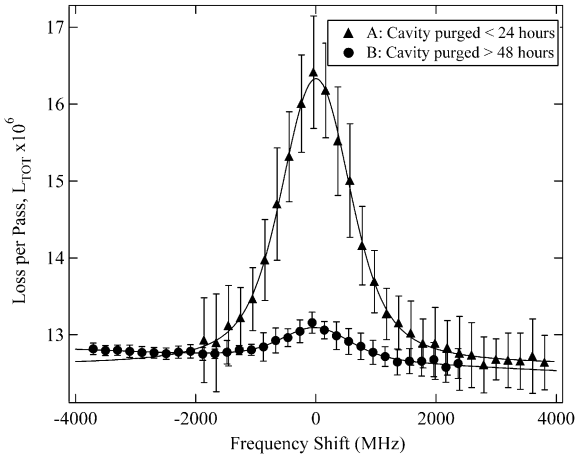

Fig. 2. CRDS spectra of background levels of water in the ring-down cavity after purging with dry nitrogen, where zero frequency shift corresponds to the center of the strong line given in Table 1. These spectra were taken in flowing nitrogen at a pressure of 13.3 kPa (100 Torr). After brief purging, the cavity contained a water mole fraction of 1.4 ± 0.2 μmol/mol, derived from CRDS spectrum *A*. With additional purging and baking of the cavity, the mole fraction of water was reduced to 0.15 ± 0.03 μmol/mol, derived from CRDS spectrum *B*. The solid lines were determined by a least-squares fit of the data to a Voigt profile with a linear baseline.

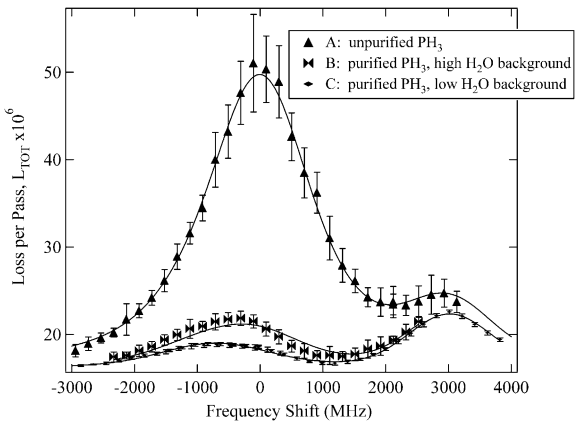

Fig. 3. CRDS spectra of purified and unpurified phosphine (from cylinder *B*) sampled under flowing conditions. Here zero frequency shift corresponds to the center of the strong H_2O line given in Table 1. Two other absorption peaks associated with the bulk phosphine occur at frequency shifts of −700 and 3000 MHz from the H_2O line center. The three spectra were fit via the method of least-squares to Eq. (2), assuming the two phosphine peaks had constant shape and size and assuming Voigt line shapes for all component peaks. The only variable between the three spectra was the size of the water absorption peak.

remeasured with this lower background water concentration: this spectrum is trace *C*, Fig. 3. Note that nearby phosphine absorption lines are convoluted with the water absorption line, a complication that also occurred with the weaker water line discussed earlier. However, having spectra with varying quantities of water and constant quantities of phosphine allows a deconvolution of these peaks according to the model given by Eq. (2).

A global fit of these three phosphine spectra requiring consistent phosphine line strengths and locations was performed as shown in Fig. 3; the only variable that differs for the three spectra is the height of the water peak. This fit yielded H_2O mole fractions of 18.0 ± 1.5, 1.6 ± 1.1, and 0.05 $(+1.0/-0.05)$ μmol/mol for unpurified phosphine, purified phosphine with relatively high background level of water, and purified phosphine with low background water, respectively. Since spectrum *C* contains so little water, the peaks visible in that spectrum are essentially due completely to the phosphine absorption lines. The uncertainties in H_2O mole fraction are roughly the same for each of the three spectra in Fig. 3 and are about five times greater than those obtained from the phosphine-free spectra of Fig. 2. This reflects the additional uncertainty associated with fitting a multi-peak spectrum that includes previously uncharacterized phosphine peaks.

However, the H_2O mole fraction for the purified phosphine corresponds well to the background levels of water measured in nitrogen immediately before the phosphine measurements. Nitrogen trace *A* of Fig. 2 shows a mole fraction of 1.4 ± 0.2 μmol/mol and was measured immediately before phosphine trace *B* of Fig. 3, which had a mole fraction of 1.6 ± 1.1 μmol/mol of water. Although phosphine trace *C* of Fig. 3 has an uncertainty of 1.0 μmol/mol for its fit mole fraction, it clearly contains less water than phosphine trace *B* of Fig. 3. According to the purifier specifications, the purified phosphine should contain less than 1 nmol/mol water. Interestingly, the H_2O mole fraction measured for the unpurified phosphine is nearly 20 times higher than the manufacturer's specification of 1 μmol/mol. Although this cylinder was fresh, it was a special "short-fill" to meet our requirements and contained less than one-third the normal amount of phosphine.

The global fit of the three phosphine spectra in Fig. 3 also allows the determination of preliminary values for the line strengths and locations of the two observed phosphine absorption lines. Phosphine absorption lines in this spectral range have not been previously described in the literature and are quite weak compared to the adjacent water line. According to the global fit, the smaller phosphine peak has a transition wavenumber of $10\,687.34 \pm 0.01\ \mathrm{cm}^{-1}$; the larger phosphine peak has a wavenumber of $10\,687.464 \pm 0.001\ \mathrm{cm}^{-1}$. The line strength for both peaks is on the order of 10^{-23} cm^2 MHz/molecule, nearly six orders of magnitude smaller than the adjacent strong water line.

To test the correlation of water in the phosphine source gas with materials properties, a layered sample of AlInP was grown by MBE as described above with the first AlInP layer grown using purified phosphine and the second layer grown using unpurified. This sample was analyzed both by photocurrent measurements [11] and with secondary-ion mass spectrometry (SIMS). The light I–V curves from the photocurrent measurements showed good material quality for both layers of the film. The current density under reverse bias and under illumination was $-0.165\ \mathrm{mA/cm^2}$ with only the GaAs cap removed and $-0.14\ \mathrm{mA/cm^2}$ with the three top layers removed. The commercially obtained SIMS results, shown in Fig. 4, show a slight difference in oxygen concentration between the two AlInP layers. The AlInP layer grown with purified phosphine contains 1.5×10^{17} O atoms/cm^3, averaged over the central part of the layer ignoring the interface effects; the AlInP layer grown with unpurified phosphine contains 1.7×10^{17} O atoms/cm^3, corresponding to an increase of 2×10^{16} O atoms/cm^3 relative to the layer grown with the purified phosphine.

The unpurified phosphine contains nearly 20 μmol/mol more H_2O than the purified phosphine but causes an increase in the O to P ratio in the resulting material of less than 1 μmol/mol (from 6.8 to 7.7 μmol/mol). While this difference is measurable, it is smaller than anticipated. This

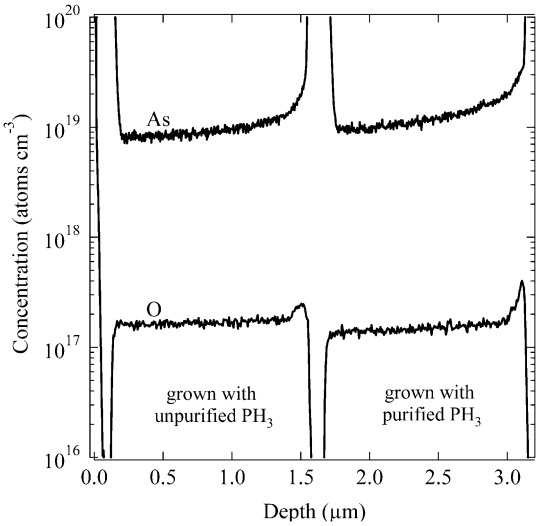

Fig. 4. SIMS results for $Al_{0.58}In_{0.42}P$ layered sample grown with phosphine from cylinder *B*. On average, the AlInP grown with purified phosphine contains an oxygen concentration of 1.5×10^{17} atoms/cm^3, while the AlInP layer grown with unpurified phosphine contains 1.7×10^{17} O atoms/cm^3. Arsenic concentrations are also shown to provide a visual guide to the layers.

phenomenon requires further study, but comparison with samples grown with characterized phosphine using organometallic vapor phase epitaxy (OMVPE) would likely exhibit greater sensitivity to residual H_2O content in the source gas. Unlike the growth process in OMVPE, in MBE the phosphine is injected into the growth chamber via a cracker at 1050°C, which may be chemically altering the water and reducing its incorporation into the growing material.

5. Summary

These measurements of residual water in bulk phosphine are the first published CRDS measurements in phosphine gas. We demonstrated the use of CRDS to quantify trace moisture levels in semiconductor source gases and subsequently investigated the material properties of semiconductors grown with well-characterized phosphine. Although the phosphine absorption lines near the water lines of interest complicate the measurements, the high spectral resolution of the CRDS technique enables deconvolution of these interferences from the water spectra. Finally, we have found water concentrations well above manufacturers' specifications for two different cylinders of phosphine, and we have measured a 1 μmol/mol increase in O to P ratio in MBE-grown $Al_{0.58}In_{0.42}P$ when an additional 20 μmol/mol of water was present in the PH_3 source gas.

In the wavelength region of 940 nm accessible with our current apparatus, the detection limit for CRDS is less than 20 nmol/mol. This value is limited mainly by the relative weakness of the water absorption lines in this region; at longer wavelengths, the H_2O absorption lines are stronger, lowering the detection limit. In the region of 1390 nm, the practical detection limit for CRDS measurements of H_2O using the apparatus described here should approach 0.3 nmol/mol. For a more recent reference discussing the cavity ringdown technique, see ref. [12].

References

[1] J.J. McAndrew, D. Boucheron, Solid State Technol. 35 (1992) 55.
[2] B.R. Stallard, L.H. Espinoza, R.K. Rowe, M.J. Garcia, T.M. Niemczyk, J. Electrochem. Soc. 142 (1995) 2777.
[3] A. O'Keefe, D.A.G. Deacon, Rev. Sci. Instrum. 59 (1988) 2544.
[4] G. Berden, R. Peeters, G. Meijer, Int. Rev. Phys. Chem. 19 (2000) 565.
[5] P.L. Varghese, R.K. Hanson, Appl. Opt. 23 (1984) 2376.
[6] R.D. van Zee, J.T. Hodges, J.P. Looney, Appl. Opt. 38 (1999) 3951.
[7] R. Schermaul, R.C.M. Learner, D.A. Newnham, R.G. Williams, J. Ballard, N.F. Zobov, D. Belmiloud, J. Tennyson, J. Mol. Spectrosc. 208 (2001) 32.
[8] R. Schermaul, R.C.M. Learner, D.A. Newnham, J. Ballard, N.F. Zobov, D. Belmiloud, J. Tennyson, J. Mol. Spectrosc. 208 (2001) 43.
[9] D.C. Hovde, J.T. Hodges, G.E. Scace, J.A. Silver, Appl. Opt. 40 (2001) 829.
[10] H.H. Funke, M.W. Raynor, B. Yücelen, V.H. Houlding, J. Electron. Mater. 30 (2001) 1438.
[11] K.A. Bertness, S.R. Kurtz, S.E. Asher, R.C. Reedy Jr., J. Crystal Growth 196 (1999) 13.
[12] J.G. Cormier, J.T. Hodges, J.R. Drummond, "On the Application of Cavity Ringdown Spectroscopy to Measurements of Line Shapes and Continuum Absorption," In: Christina A. Back (Ed.), Spectral Line Shapes: 16th International Conference on Spectral Line Shapes (Volume 12), AIP Conference Proceedings 645, 2002, pp. 401–412.